Theory of the spin relaxation of conduction electrons in silicon

J. L. Cheng,[1,2] M. W. Wu,[1] and J. Fabian[2,*]

[1] *Hefei National Laboratory for Physical Sciences at Microscale and Department of Physics, University of Science and Technology of China, Hefei, Anhui, 230026, China*

[2] *Institute for Theoretical Physics, University of Regensburg, 93040 Regensburg, Germany*

A realistic pseudopotential model is introduced to investigate the phonon-induced spin relaxation of conduction electrons in bulk silicon. We find a surprisingly subtle interference of the Elliott and Yafet processes affecting the spin relaxation over a wide temperature range, suppressing the significance of the intravalley spin-flip scattering, previously considered dominant, above roughly 120 K. The calculated spin relaxation times T_1 agree with the spin resonance and spin injection data, following a T^{-3} temperature dependence. The valley anisotropy of T_1 and the spin relaxation rates for hot electrons are predicted.

PACS numbers: 72.25.Rb, 72.25.Dc, 76.30.Pk

Silicon is the core material for the information technology. Yet we know surprisingly little about the spin relaxation processes of its conduction electrons [1, 2]. With the pioneering demonstration of the spin injection into silicon by Appelbaum et al. [3, 4] and related experimental breakthroughs [5, 6] and steps towards silicon spintronics [7], as well as with theoretical analyses [8, 9, 10], we have gained valuable new insight into the spin transport and relaxation in this material.

A systematic investigation of the conduction electron spin relaxation time T_1 in silicon was conducted earlier by Lépine [11] using electron spin resonance (ESR) (see the summary in Ref. 2). As the ESR does not discriminate between conduction electrons and electrons bound on donors, the representative data are limited to temperatures above $T \approx 150$ K at which most electrons are in the conduction band for the investigated donor densities [11]. Spin injection, on the other hand, looks at conduction electrons only. Appelbaum et al. [3, 6] extracted useful data below 150 K, filling the gap. These measurements were using samples with nondegenerate electron densities. The conduction electron spin relaxation and spin transport properties were also investigated in Si/SiGe quantum wells [10, 12]. There, however, the spin coherence is due not to the bulk-derived properties, but rather due to the appearance of the structure-inversion anisotropy spin-orbit fields.

While it is generally believed that the spin relaxation in silicon is caused by the Elliott-Yafet mechanism [2, 3, 6, 11, 13] (unlike in III-V semiconductors, in which the most important mechanism is the D'yakonov-Perel' one [14]) there is yet no systematic theoretical study of it. There are two processes involved: that of Elliott and Yafet. In the Elliott processes [15] the spin-flip is due to the admixture of the Pauli up and down spins in the Bloch state, caused by spin-orbit coupling. The electron-phonon matrix element couples only equal Pauli spins. In the Yafet processes [13] spin flips are due to the phonon-modulated spin-orbit coupling so that the electron-phonon coupling alone couples opposite spins. The two processes interfere destructively at low phonon momenta affecting T_1 typically at very low temperatures [13]. Yafet gave qualitative estimates for T_1 in silicon assuming intravalley electron-acoustic phonon scattering, finding that $T_1 \sim T^{-5/2}$. This temperature dependence has been widely used to fit experimental data [2, 3, 6, 11, 16].

Here we perform comprehensive theoretical investigation of T_1 in bulk silicon within the Elliott-Yafet mechanism. We introduce a pseudopotential model that reproduces the known spin-orbit splittings of the relevant electronic states. The model, together with a realistic phonon structure taken from the adiabatic bond charge model [17], allows us to calculate the spin mixing probabilities and the electron-phonon-induced spin flips for both the Elliott and Yafet processes. We show that the interference between the two processes affects T_1 over a remarkably wide temperature range. Both the intra and intervalley spin-flip scatterings are important [optical (OP) phonons are less relevant than acoustic (AC) ones] making Yafet's prediction invalid. Our calculated $T_1(T)$, which is in quantitative agreement with experiment, is well described by the $T_1 \sim T^{-3}$ dependence. We further predict the valley anisotropy of T_1 and give the spin relaxation rates for hot electrons.

The presence of space inversion symmetry in bulk silicon allows to write the Bloch states as combinations of the Pauli spinors [2, 13],

$$|\mathbf{k}, n \Uparrow\rangle = \sum_{\mathbf{g}} \left[a_{\mathbf{k},n}(\mathbf{g})|\uparrow\rangle + b_{\mathbf{k},n}(\mathbf{g})|\downarrow\rangle\right]|\mathbf{k}+\mathbf{g}\rangle \ , \quad (1)$$

$$|\mathbf{k}, n \Downarrow\rangle = \sum_{\mathbf{g}} \left[a^*_{\mathbf{k},n}(\mathbf{g})|\downarrow\rangle - b^*_{\mathbf{k},n}(\mathbf{g})|\uparrow\rangle\right]|\mathbf{k}+\mathbf{g}\rangle \ . \quad (2)$$

Here $\mathbf{k}$ is the lattice momentum confined to the first Brillouin Zone, n is the band index, $\Uparrow(\Downarrow)$ is the effective spin index, $\mathbf{g}$ denote the reciprocal lattice vectors, and $|\mathbf{k}\rangle$ stand for the plane waves. The two states above are degenerate, and can so be chosen as the spin "up" and "down" states to satisfy $\langle \mathbf{k}, n \Uparrow |\sigma_z| \mathbf{k}, n \Downarrow\rangle = 0$. The mixing of the Pauli spins in the spin "up" ("down") state is

characterized by the mixing probability $|b_{\mathbf{k},n}|^2$, which is key to understand spin relaxation.

We follow the scheme of Ref. [18] and build a pseudopotential model incorporating spin-orbit coupling to obtain the electronic states and electron-phonon coupling needed to calculate T_1. The pseudopotential of each atom is the sum of the scalar (v_n) and spin-orbit ($v_{\rm so}$) parts, $v(\mathbf{r}) = v_n(\mathbf{r}) + v_{\rm so}(\mathbf{r})$; the form factors are $v(\mathbf{k}_1,\mathbf{k}_2) = \int (d^3\mathbf{r}/a^3) e^{-i(\mathbf{k}_1-\mathbf{k}_2)\cdot\mathbf{r}} v(\mathbf{r})$, with the lattice constant $a = 5.431$ $\mathring{A}$. The scalar part $v_n(\mathbf{r})$ is taken from Ref. [19], reproducing well the silicon bands. We introduce the spin-orbit part as [20, 21] $v_{\rm so}(\mathbf{r}) = \lambda\theta(r-r_c)\hat{\mathbf{L}}\cdot\hat{\boldsymbol{\sigma}}\mathcal{P}_1$, where $\hat{\mathbf{L}}$ is the angular momentum operator, $\mathcal{P}_l$ is the projector on the orbital momentum state l, $r_c = 2r_B$ is the effective radius for the spin-orbit coupling (r_B is the Bohr radius), and λ is a spin-orbit parameter to be fitted to the valence band spin-orbit splitting Δ^l_{25}. The fitted form factor of $v_{\rm so}$ can be approximated by [21] $v_{\rm so}(\mathbf{k}_1,\mathbf{k}_2) = -i\Delta_{\rm so}(a/2\pi)^2 \mathbf{k}_1\times\mathbf{k}_2\cdot\boldsymbol{\sigma}$, with the effective spin-orbit interaction $\Delta_{\rm so} = (16\pi^3/45)(r_c/a)^5\lambda = 9.475\times10^{-4}$ eV. The actual spin-orbit pseudopotential Hamiltonian matrix element comprises the structure and form factors: $\langle\mathbf{k}_1|H_{\rm so}|\mathbf{k}_2\rangle = \cos[(\mathbf{k}_1-\mathbf{k}_2)\cdot\boldsymbol{\tau}] v_{\rm so}(\mathbf{k}_1,\mathbf{k}_2)$, where $\boldsymbol{\tau} = (a/8)(1,1,1)$. The pseudopotential Hamiltonian is diagonalized on a basis of 387 plane-waves, large enough to converge the spin mixing probabilities around the conduction band edge. The sums over momenta are performed using the tetrahedron method.

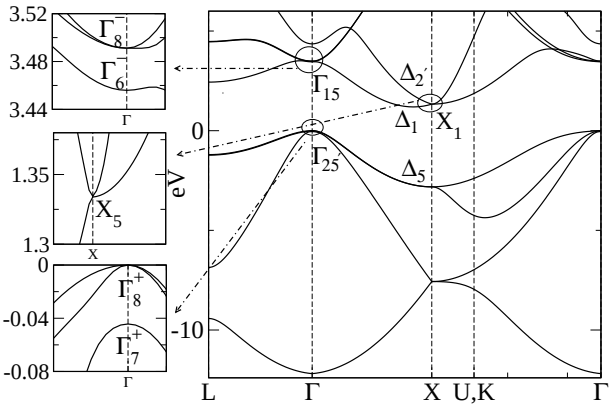

FIG. 1: Calculated electronic band structure of silicon. The single group notation [22] is used in the main plot, while the double group notation [23] appears on the zoom plots.

The calculated electronic band structure is shown in Fig. 1; Table I displays selected band-structure properties, calculated and measured. The agreement with known data is very satisfactory, justifying our pseudopotential for exploring spin-orbit effects in silicon. In the following we denote the wave vectors of the six conduction-band valleys as $\mathbf{K}_i$, with $i = X(\bar{X})/Y(\bar{Y})/Z(\bar{Z})$ standing for the corresponding valley orientation.

Let us first see what can we learn about b^2 from symmetry group arguments. Consider the Z valley and take the spin-orbit interaction $H_{\rm so} \propto L_x\sigma_x + L_y\sigma_y + L_z\sigma_z$ as a perturbation. Group theory shows that the conduction band (Δ_1, see Fig. 1) couples only to the the valence band (Δ_5) at the band edge, so that the spin mixing is of the order of $|b_{ck}|^2 \approx (\Delta_{\rm so}/E_g)^2 \sim 10^{-6}$ [13, 15]. In addition to the magnitude, we can also learn about the valley anisotropy of b^2. We can describe the symmetry character of the conduction band orbital states as $|Z\rangle$, and that of the degenerate valence states as $|X\rangle/|Y\rangle$ [23], in the usual $\mathbf{k}\cdot\mathbf{p}$ theory sense. The only nonvanishing matrix elements of the orbital momentum between these states are $\langle X|L_y|Z\rangle = -\langle Y|L_x|Z\rangle$, by symmetry. Therefore, the effective spin-orbit interaction involves only the σ_x and σ_y terms with equal contribution. If the spin is quantized along z, both σ_x and σ_y terms contribute equally to the spin mixing b^2. However, only one of them, *i.e.*, σ_y/σ_x term, contributes to the spin mixing for the x/y quantized spin. Since the spin along x/y for the Z valley is equivalent to the spin along z for the X/Y valley under a $\frac{\pi}{2}$-rotation around the y/x axis, we can conclude that the average spin mixing is anisotropic with respect to the valley orientation: $\langle b^2\rangle_{\epsilon,Z} \approx 2\langle b^2\rangle_{\epsilon,X/Y}$. This is indeed found from numerics, as shown in Fig. 2. See EPAPS Document No. for a more intuitive explanation of the anisotropy.

Unit	eV			meV		m_0		ΓX
	$E_{\Gamma_{15}}$	E_{X_1}	E_g	Δ^l_{25}	Δ_{15}	m_l^Δ	m_t^Δ	$k_{\rm min}$
Exp. [24]	3.4	1.25	1.17	44	30-40	0.9163	0.1905	
Cal.	3.46	1.33	1.19	44	35	0.915	0.204	0.846

TABLE I: Comparison between measured and calculated band-structure characteristics. Displayed is the energy $E_{\Gamma_{15}}$ of the direct gap at Γ_{15}, the energy E_{X_1} of the X_1 (X_5) point, and the indirect band gap E_g. The spin-orbit split off energy of the top of the valence band is Δ^l_{25}, and that of the conduction band Γ_{15} point is Δ_{15} (the stated range of values are calculated [24]). Further shown are the longitudinal (m_l^Δ) and transverse (m_t^Δ) effective masses (in the units of the free electron mass) at the conduction band minimum at $k_{\rm min}$ along the Δ lines ΓX.

Figure 2 also shows a peak around 150 meV, which is roughly the energy of X_1. This peak indicates a large spin mixing on the X plane. In the X plane, there is anticrossing along the X-W direction due to spin-orbit coupling of degenerate bands Δ_1 and Δ_2', which results in large spin mixing (similar to spin hot spots [20]). The anticrossing is absent at the X-point, but grows along the X-W direction to the order of $\frac{1}{2}$ quickly. See EPAPS Document No. for more details on spin hot spots in silicon. In the inset of Fig. 2, we also plot the temperature dependence of the average spin mixing $\langle b^2\rangle_{T,i} = \sum_{\mathbf{k}\in i}|b_{c\mathbf{k}}|^2 f(\varepsilon_{\mathbf{k}})/\sum_{\mathbf{k}\in i} f(\varepsilon_{\mathbf{k}})$, where $f(\varepsilon_{\mathbf{k}}) = Ce^{\varepsilon_{\mathbf{k}}/(k_BT)}$ is the properly normalized (C) Maxwell-Boltzmann distribution. The anisotropy,

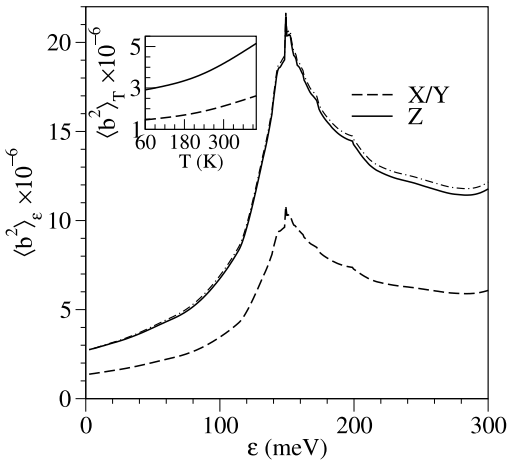

FIG. 2: Calculated energy dependence of the spin mixing probability $\langle b^2\rangle_\epsilon$ in the X/Y (dashed) and Z (solid) valleys. The dot-dashed curve is $2\langle b^2\rangle_{\epsilon,X}$. The inset shows the temperature dependent $\langle b^2\rangle_T$.

$\langle b^2\rangle_{T,Z} \approx 2\langle b^2\rangle_{T,X/Y}$, remains.

The spin-flip electron-phonon matrix elements for the conduction states $|\mathbf{k}_1; c\Uparrow\rangle$ and $|\mathbf{k}_2; c\Downarrow\rangle$ are [13]

$$M^\lambda(\mathbf{k}_1,\mathbf{k}_2) = -i\sqrt{\frac{\hbar}{\rho\Omega^\lambda_{\mathbf{q}}}}\sum_{\mathbf{g}_1\mathbf{g}_2}\left[\Delta\mathbf{k}\cdot\sum_\alpha \boldsymbol{\xi}^\lambda_{\mathbf{q},\alpha}e^{-i\Delta\mathbf{k}\cdot\boldsymbol{\tau}_\alpha}\right] \times \begin{pmatrix} a_{\mathbf{k}_1,c}(\mathbf{g}_1)\\ b_{\mathbf{k}_1,c}(\mathbf{g}_2)\end{pmatrix}^\dagger v(\mathbf{k}_1+\mathbf{g}_1,\mathbf{k}_2+\mathbf{g}_2)\begin{pmatrix} -b^*_{\mathbf{k}_2,c}(\mathbf{g}_2)\\ a^*_{\mathbf{k}_2,c}(\mathbf{g}_2)\end{pmatrix}, \quad (3)$$

where $\mathbf{q} = \mathbf{k}_1 - \mathbf{k}_2$ is the phonon wave vector, $\boldsymbol{\tau}_\alpha = \pm\boldsymbol{\tau}$ are the position vectors of the two basis atoms, $\Delta\mathbf{k} = \mathbf{k}_1 + \mathbf{g}_1 - \mathbf{k}_2 - \mathbf{g}_2$, ρ is the silicon density, and $\hbar\Omega^\lambda_{\mathbf{q}}$ and $\boldsymbol{\xi}^\lambda_{\mathbf{q},\alpha}$ are the phonon energy and the polarization vector for the αth atom, obtained here from the adiabatic bond-charge model [17]. For the Elliott processes $v = v_n$, while for Yafet processes $v = v_{\rm so}$ in Eq. (3).

The spin relaxation rate is given by $T_1^{-1}(T) = \sum_{i,j} T^{-1}_{1,ij}$, with

$$T^{-1}_{1,ij}(T) = \sum_\lambda \int d\epsilon \Gamma^\lambda_{ij}(\epsilon,T) f(\epsilon). \quad (4)$$

Here Γ^λ_{ij} is the total scattering rate for the electrons of energy ϵ making λ-phonon assisted spin-flip transitions from the ith to the jth valley. For non-degenerate electron densities,

$$\Gamma^\lambda_{ij}(\epsilon,T) = \frac{4\pi}{\hbar}\sum_{\mathbf{k}_1\in i}\delta(\varepsilon_{c\mathbf{k}_1}-\epsilon)\sum_{\mathbf{k}_2\in j}\sum_\pm |M^\lambda(\mathbf{k}_1,\mathbf{k}_2)|^2 \times (\bar n_{\mathbf{q}\lambda}+\frac{1}{2}\pm\frac{1}{2})\delta(\varepsilon_{c\mathbf{k}_2}-\epsilon\pm\Omega_{\mathbf{q}\lambda}), \quad (5)$$

where $\bar n_{\mathbf{q},\lambda}$ is the phonon distribution. Considering the low-energy intravalley processes with AC phonons Yafet found the dependence of $T_1^{\rm intra} \sim T^{-5/2}$ [13]. That prediction was based on Yafet's observation that the time reversal and space inversion symmetry inhibits the low momentum scattering, expressed in the quadratic dependence, $M^\lambda(\mathbf{k}_1,\mathbf{k}_2) \propto |\mathbf{q}|^2/\sqrt{\Omega^\lambda_{\mathbf{q}}}$, valid for low $\mathbf{q}$.

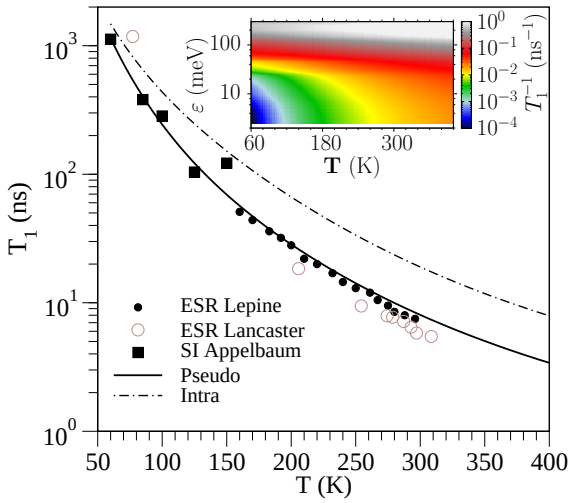

FIG. 3: Spin relaxation time in silicon as a function of temperature. The solid curve is the calculation, the symbols are the spin injection (Appelbaum) [3, 25] and the electron spin resonance (Lepine and Lancaster) [11, 16] data (see Ref. 2). The dashed-dotted curve is $T_1^{\rm intra}$ of the intravalley scattering only. The inset shows the contour plot of the spin relaxation rate T_1^{-1} of hot electrons, as a function of the electron energy ε and lattice temperature T.

Our main result is in Fig. 3 which shows the calculated $T_1(T)$. The agreement with experiments [2, 3, 11, 16] is very good. Clearly, the intravalley spin relaxation $T_1^{\rm intra}$ alone is not sufficient to explain the experiment. While there is no single scattering type governing the whole temperature range, precluding a simple theoretical prediction for $T_1(T)$, a fit to the numerical data gives $T_1 \sim T^{-3}$ in the investigated temperature region. Considering intravalley processes only, Yafet's prediction $T_1^{\rm intra} \propto T^{-5/2}$ works at low T. Due to the strong spectral dependence (peak) of $\langle b^2\rangle_\epsilon$ more energetic electrons at higher temperatures strongly bias the average spin relaxation, making $T_1^{\rm intra}(T)$ decay faster than predicted. This behavior is also reflected in the energy-resolved spin relaxation rate, shown in the inset to Fig. 3. The strong increase of the rate with increasing energy is due to the increase in the scattering phase space and b^2.

Figure 4 gives a comprehensive analysis of the calculated T_1. The comparison of the AC and OP phonon contributions as well as the intra and intervalley contributions to spin relaxation is shown in Fig. 4(a). We find that the spin relaxation is dominated by intravalley electron-AC phonon scattering at low temperatures ($T \lesssim 120$ K), and by intervalley electron-AC phonon scattering at high temperatures ($T \gtrsim 120$ K). Figure

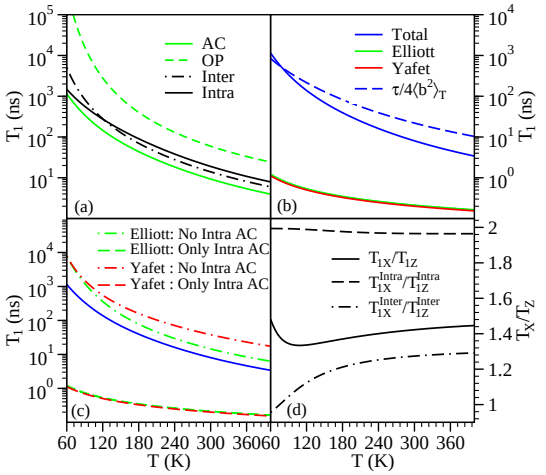

FIG. 4: Analysis of the spin relaxation in silicon. (a) Spin relaxation time induced by acoustic (green solid) and optical (green dashed) phonons, as well as by intervalley (dash-dotted) and intravalley (solid) scattering. (b) Elliott (green) and Yafet (red) processes compared to the total T_1 (blue). The estimate based on the knowledge of the momentum relaxation time τ and b^2 is also indicated (dashed blue). (c) Elliott and Yafet processes with and without intravalley acoustic phonons. The blue curve is the total T_1. (d) Valley-anisotropy ratios T_{1X}/T_{1Z} (solid); intravalley (dashed) and intervalley (dot-dashed) scattering are distinguished.

4(b) resolves the individual contributions of the Elliott and Yafet processes. Remarkably, they would individually lead to T_1 orders of magnitude below the actual spin lifetime, over the whole temperature range! The destructive interference of the two processes is a very subtle effect (also in terms of numerics). The fact that the Elliott and Yafet processes interfere destructively was predicted already by Yafet on symmetry grounds [13]. See EPAPS Document No. for more details. The same figure also brings the estimated spin relaxation time using the conventional formula [18, 20] $T_1 = \tau/4\langle b^2\rangle_T$, where τ is the momentum relaxation time calculated from our pseudopotential model. This estimate fails in silicon especially at high temperatures. The subtle nature of the interference between the Elliott and Yafet processes is displayed in Fig. 4(c). Each process is dominated by the the intravalley electron-AC phonon scattering over all temperatures. The interference drastically reduces the significance of this scattering. One consequence of our calculation would be the decrease of the Elliott-Yafet T_1 in silicon structures with reduced spatial inversion symmetry (gated, for example), since in such cases the interference could be gradually removed. A recent experiment indeed finds a dramatic reduction of the spin relaxation time in Si/SiO_2 interfaces compared to the bulk [26].

Finally, we explore the anisotropy of T_1 with respect to the valley orientation. Figure 4(d) gives the ratio T_{1X}/T_{1Z} resolved for the intra and intervalley scattering. Assuming that the anisotropy of T_1 comes mainly from the spin mixing, that is, $T_{1,ij}^{-1} \propto \sqrt{\langle b^2\rangle_{T,i}\langle b^2\rangle_{T,j}}$, we get $T_{1X}^{\mathtt{intra}}/T_{1Z}^{\mathtt{intra}} \approx 2$, as well as $T_{1X}^{\mathtt{inter}}/T_{1Z}^{\mathtt{inter}} \approx 4-2\sqrt{2}$ for intervalley f-processes (non-opposite valleys), and $T_{1X}^{\mathtt{inter}}/T_{1Z}^{\mathtt{inter}} \approx 2$ for g-processes (opposite valleys). These estimates agree with our numerical results. The predicted anisotropy could be tested in strained silicon with lifted valley degeneracy.

In summary, we explained the measured spin relaxation in silicon performing realistic pseudopotential calculations of the Elliott-Yafet mechanism. We found the dominant scattering processes and their temperature dependence, predicted the valley anisotropy as well as T_1 for hot electrons.

This work was supported by DFG SPP1285, GRK 638, the Natural Science Foundation of China under Grant No. 10725417, the National Basic Research Program of China under Grant No. 2006CB922005, and the Knowledge Innovation Project of the Chinese Academy of Sciences. J.L.C was partially supported by China Postdoctoral Science Foundation. We thank C. Ertler and M. Q. Weng for valuable discussions.

* Author to whom correspondence should be addressed; Electronic address: jaroslav.fabian@physik.uni-regensburg.de

[1] I. Žutić, J. Fabian, and S. Das Sarma, Rev. Mod. Phys. **76**, 323 (2004).
[2] J. Fabian, A. M. Abiague, C. Ertler, P. Stano, and I. Žutić, Acta Physica Slovaca **57**, 565 (2007).
[3] I. Appelbaum, B.Q. Huang, and D. J. Monsma, Nature, **447**, 295 (2007).
[4] I. Žutić and J. Fabian, Nature (London) **447**, 269 (2007).
[5] B. T. Jonker, G. Kioseoglou, A. T. Hanbicki, C. H. Li, and P. E. Thompson, Nature Phys. **3**, 542 (2007).
[6] B.Q. Huang, D. J. Monsma, and I. Appelbaum, Phys. Rev. Lett. **99**, 177209 (2007).
[7] B. Min, K. Motohashi, C. Lodder, and R. Jansen, Nature Mater. **5**, 817 (2006).
[8] I. Žutić, J. Fabian, and S. C. Erwin, Phys. Rev. Lett. **97**, 026602 (2006).
[9] P. Mavropoulos, Phys. Rev. B 78, 054446 (2008).
[10] P. Zhang and M. W. Wu, Phys. Rev. B **79**, 075303 (2009).
[11] D. J. Lépine, Phys. Rev. B **2**, 2429 (1970).
[12] A. M. Tyryshkin, S. A. Lyon, W. Jantsch, and F. Schäffler, Phys. Rev. Lett. **94**, 126802 (2005).
[13] Y. Yafet, in *Solid State Physics*, edited by F. Seitz and D. Turnbull (Academic, New York, 1963), Vol. **14**, p. 1.
[14] J. H. Jiang and M. W. Wu, Phys. Rev. B **79**, 125206 (2009).
[15] R. J. Elliott, Phys. Rev. **96**, 266 (1954).
[16] G. Lancaster, J. A. V. Wyk, and E. E. Schneider, Proc. Phys. Soc. **84**, 19 (1964).
[17] W. Weber, Phys. Rev. B **15**, 4789 (1977).
[18] J. Fabian and S. D. Sarma, Phys. Rev. Lett. **83**, 1211 (1999).
[19] J. R. Chelikowsky and M. L. Cohen, Phys. Rev. B **10**, 5095 (1974);Phys. Rev. B **14**, 556 (1976).

[20] J. Fabian and S. D. Sarma, Phys. Rev. Lett. **81**, 5624 (1998).
[21] G. Weisz, Phys. Rev. **149**, 504 (1966).
[22] M. Cardona and F. H. Pollak, Phys. Rev. **142**, 530 (1966).
[23] Peter Y. Yu and M. Cardona, *Fundamentals of Semiconductors: Physics and Materials Properties* (Springer Berlin Heidelberg New York, 2005).
[24] Physics of Group IV Elements and III-V Compounds, edited by O. Madelung, Landolt-Bornstein: *Numerical Data and Functional Relationships in Science and Technology*, Group III (Springler-Verlag, Berlin, 1982), Vol. **17a**.
[25] We used revised spin injection data (B. Huang and I. Appelbaum, unpublished). In the original publication the spin relaxation was obtained by using $P \propto (I^P_{C2} - I^{AP}_{C2})/I_{C1}$ for the spin polarization (the notation applies to Ref. 3), to make the most conservative lifetime estimate possible. The revised data were extracted using the conventional definition $P = (I^P_{C2} - I^{AP}_{C2})/(I^P_{C2} + I^{AP}_{C2})$. We are indebted to I. Appelbaum for this communication.
[26] H.-J. Jang and I. Appelbaum, Phys. Rev. Lett. **103**, 117202 (2009).